

ANALYSIS OF NATURAL CONVECTION IN HORIZONTAL CONCENTRIC ANNULI OF VARYING INNER SHAPE

Xing Yuan, Fatemeh Tavakkoli, and Kambiz Vafai

Department of Mechanical Engineering, University of California, Riverside, CA, USA

An investigation is presented of free convection in horizontal concentric annuli of varying with inner shape where the inner and outer surfaces are kept at a constant temperature. The simulation is categorized into four groups based on the shape of the inner entity, which is either cylindrical, elliptical, square, or triangular. Flow and thermal fields are exhibited by means of streamlines and isotherms. Overall heat transfer correlations incorporating thermal radiation are established and presented in terms of the Nusselt number. It is observed that the surface radiation and presence of corners and larger top space enhances the heat transfer rate. As the reference temperature increases, surface radiation plays a more prominent role in the overall heat transfer performance.

1. INTRODUCTION

Natural convection heat transfer within an annulus has been a subject of interest for decades. Natural convection in a finite space is important for many applications, including the design of electronic equipment cooling systems, nuclear reactor waste transport and storage, solar collectors and thermal storage systems, and thermal management of aviation.

Natural convection in an enclosure can vary quite substantially due to the geometry of the enclosure. There are a significant number of reported experimental, analytical, and numerical studies in the literature on natural convection in an annulus with different boundary conditions. These articles address the effects of Rayleigh number, Prandtl number, the influence of different media, the influence of different inner and outer boundary shapes, the ratio of gap width to inner characteristic diameter, and the effect of inclination angle and eccentricity [1–17].

Angeli et al. [1] described the evolution of flow regimes and temperature patterns within a horizontal annulus with increasing values of Rayleigh number. For very low Raleigh number (Ra) values, the regime is pseudo-diffusive and the heat transfer process is conduction dominated. Such a regime persists providing the annular gap, L and/or the temperature difference between the inner and outer walls are/is sufficiently small. Numerical calculations were also performed by Ho et al. [2] for an

Received 8 August 2014; accepted 25 January 2015.

Address correspondence to Kambiz Vafai, Department of Mechanical Engineering, University of California, Riverside, CA, 92521, USA. E-mail: Vafai@engr.ucr.edu

NOMENCLATURE

A	surface area for heat transfer	q	local heat flux, W/m^2
α	thermal diffusivity, m^2/s	Q	overall heat flux, W/m
D	diameter	Ra	Raleigh number = $\frac{g\beta(T_i - T_o)L^3\rho}{\alpha\mu}$
β	thermal expansion coefficient, $1/\text{K}$	T	temperature, K
g	gravitational acceleration, m/s^2	T_0	reference temperature = $(T_i + T_o)/2$, K
ε	average emissivity	u, v	velocities in the x - and y -directions
Gr	Grashof number		
μ	viscosity, $\text{kg}/(\text{m} \cdot \text{s})$	Subscripts	
k	thermal conductivity, $\text{W}/(\text{m} \cdot \text{K})$	i	inner
ρ	density, kg/m^3	o	outer
K_{eq}	equivalent conductivity	0	reference quantities
θ	angular coordinate	c	convection
L	equivalent annulus gap width	r	radiation
Nu, \overline{Nu}	local and average Nusselt number	Superscripts	
P	pressure, Pa	*	dimensionless quantities
Pr	Prandtl number		

annulus with a radius ratio fixed at 2.6 to investigate the effect of variations in Ra and Prandtl number, Pr on the fluid flow pattern and heat transfer rate. Their work was based on steady laminar two-dimensional natural convection in cylindrical annuli with constant heat flux on the inner wall and isothermal temperature on the outer wall. They showed that the influence of Pr is quite weak and that the heat and fluid flows are primarily dependent on Ra number and the eccentricity of the annulus. In this work, we set Pr at a specified value based on the reference temperature, T_0 , and focused on investigating the influence of Ra and Radiation effects.

Shu et al. [3] demonstrated the effects of the eccentricity of the inner cylinder on the local and overall heat transfer coefficients. It was found that global recirculation, flow separation, and the space between the two cylinders had significant effects on plume inclination and that the overall heat transfer improved with eccentricity except in the middle region, where the overall Nusselt number remained at the same level as that for the concentric case.

The effects of thermal radiation on natural convection were investigated by Han and Baek [4] and Shaija and Narasimham [5]. The working medium was assumed to be homogeneous and gray. It was found that the radiation effect resulted in a more uniform temperature distribution, which reduced the convective heat transfer while the average heat transfer rate was enhanced due to the radiation effect. Tan and Howell [6] discussed the influences of radiation–conduction parameter, Rayleigh number, and other parameters on flow and temperature distributions and heat transfer in a two-dimensional participating square medium.

The effect of radiation on natural convection is typically more prominent than the forced convection case due to the coupling between temperature and flow fields in natural convection. Akiyama and Chong [7] investigated a model for prediction of the influence of gray surface radiation on natural convection in a square enclosure. It was found that the Nusselt number for natural convection with surface radiation can be expressed as a function of Ra and emissivity, ε as $Nu = 0.529 Ra^{0.3065} \varepsilon^{0.3497}$.

There are several articles on natural convection within annuli of varying shape boundary. Sambamurthy et al. [8] performed a numerical study of two-dimensional conjugate natural convection in a horizontal cylindrical annulus between an inner heat-generating solid square element and an outer isothermal circular boundary. Correlations were developed for estimating various quantities of interest for different configurations, and thermal conductivity and aspect ratios.

Xu et al. [9] investigated laminar natural convective heat transfer of air within a horizontal annulus between a heated triangular element and its circular cylindrical outer enclosure. They demonstrated the influence of Rayleigh number, radius ratio, and inclination angle on stream function and local and average Nusselt numbers. It was found that the inclination angle of the inner triangular cylinder had a negligible effect on average Nusselt number at a constant radius ratio. Xu et al. [10] also investigated an annulus composed of a horizontal cylinder inside a concentric triangular enclosure. They found that the overall heat transfer rate was independent of the inclination angle and the geometrical cross section even though the flow patterns were substantially modified.

Yu et al. [11] investigated the effect of Pr on laminar convection from a horizontal triangular element to its concentric cylindrical enclosure. They showed that temperature distribution was almost independent of Pr value when $Pr \geq 0.7$, especially at lower Ra numbers.

Boyd [12] experimentally studied steady natural convective heat transfer across an annulus with an inner hexagonal cylinder and an outer concentric circular cylinder. Their model was based on a liquid metal fast-breeder reactor spent fuel subassembly inside a shipping container. The correlation for mean Nusselt number at the surface of the inner cylinder was expressed as $\bar{Nu} = 0.794 Ra_R^{0.25}$. They showed that the presence of inner hexagonal element corners, as compared with an inner circular cylinder, enhanced the mean heat transfer.

Shu et al. [13] numerically studied natural convective heat transfer in a horizontal eccentric annulus between a square outer enclosure and a heated circular inner cylinder. It was found that flow separation at the top space between the square outer enclosure and the circular inner cylinder has a significant effect on plume inclination. Natural convection between a concentrically heated horizontal circular and cooled square enclosure was numerically studied by Moukalled [14]. The local Nusselt number along the inner wall displayed a flat trend while that along the outer surface had a peak near the top, which was different from that in a cylindrical annulus under the same conditions. Free convection in a vertical or inclined annulus has also been investigated by many authors, including Keyhani et al. [15, 16].

Transient natural convection between two horizontal isothermal cylinders was investigated by Tsui and Tremblay [17]. In most cases, the transition time from the transient to the steady state was found to be very short in comparison with typical operational times. Vafai and Etefagh [18] explored a transient three-dimensional buoyancy-driven flow inside a horizontal annulus. They found that the temperature distribution remained unchanged in the central region provided that the annulus length to outer radius ratio was over a critical value.

Aside from steady flow, Desai and Vafai [19] simulated the turbulent flow region in a horizontal cylindrical annulus. They found a core region over a

substantial length of the cavity which can be simplified into a two-dimensional model. Vafai and Desai [20] also compared the finite-element and finite difference methods in simulating natural convection in annular cavities. It was shown that the finite-element method yielded results matching those of the refined finite difference method.

There have been a significant number of investigations related to natural convection in an annulus. However, the effect of different inner shapes with or without surface radiation at relatively higher Rayleigh numbers ($\geq 10^5$) has not been established. As such, the present work addresses the effect of inner shape, which has pertinent practical applications, on flow pattern and heat transfer distribution.

2. FORMULATION

The geometry under consideration is composed of a horizontal annular region between an outer circular cylinder and inner elements of varying shape, the latter concentrically placed within the former as shown in Figure 1.

The outer cylinder and inner element are sufficiently long in the axial direction that the end effects can be ignored. In our work, both the inner and outer surfaces of the annular region are assumed to be isothermal. This is equivalent to assuming a high thermal conductivity for both inner and outer surfaces. This isothermal approximation is realistic when the thermal conductivity of both surfaces is at least one order of magnitude higher than that of air [17].

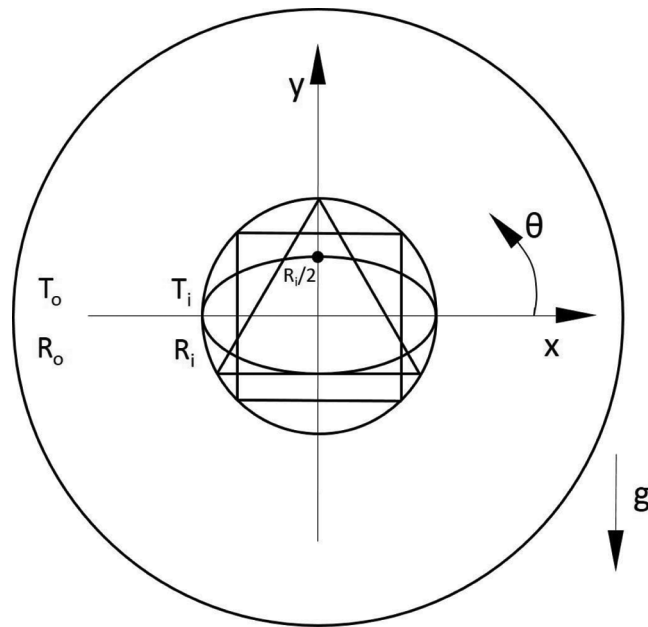


Figure 1. Concentric annuli of varying shape. (a) Local equivalent conductivity along the inner and outer surfaces. (b) Dimensionless radial temperature.

Table 1. Reference fluid properties

T_0 [K]	P_0 [atm]	$\alpha \times 10^6$ [kg/(m·s)]	$\mu \times 10^6$ [kg/(m·s)]	ρ [kg/m ³]	$\beta \times 10^3$ [1/K]
293	1	21.4	18.1	1.205	3.41
573	1	71.6	29.7	0.615	1.75
1273	1	245.9	49.0	0.277	0.79

Table 2. Grid independence test performed at $T_0 = 573$ K, $Pr = 0.674$ and $Ra = 10^6$

Number of elements	Average Nu	Deviation (%)
6,600	7.6151	5.2
8,600	7.8423	2.3
10,000	7.9327	1.2
12,000	7.9957	0.4
17,000	8.0221	0.1
26,000	8.0328	<0.001

The inner and outer surfaces are maintained at different constant temperatures. Both walls are assumed to be diffuse gray emitters and reflectors, while the intervening fluid is assumed to be a non-participating medium. All physical properties of the intervening medium are assumed to be constant and evaluated at a reference temperature of $\frac{T_i + T_o}{2}$, except for the density in the buoyancy term which is expressed using the Boussinesq approximation. The reference fluid properties are presented in Table 1. The viscous dissipation and compressibility effects are considered to be negligible.

At higher Ra values, it is important to formulate a good initial guess and a well-built mesh. We implemented the first of these requirements by applying a parametric solver which set a prior solution at a lower Ra value as the initial guess for the higher Ra value. The iterative process was tuned for a fast, efficient solution using dimensionless parameters. A well-tuned mesh helps in the convergence of the iterative process. We utilized the triangular free mesh elements in COMSOL. Typically, the free mesh is more robust for natural convection problems because COMSOL automatically refines the mesh at the corners of the domain to capture the boundary layer effects, resulting in faster convergence.

In order to determine the proper number of elements which would result in a higher accuracy and reasonable computational time, a grid independence test was performed at $T_0 = 573$ K and $Ra = 10^6$. The results of this test are given in Table 2. We chose at least 12,000 elements for all of our runs based on the results in Table 2.

2.1. Governing Equations

The choice of a proper characteristic velocity is helpful in non-dimensionalizing the governing equations. For weakly coupled systems, the characteristic velocity is usually based on free stream velocity. For buoyancy-driven flows, we chose a viscous diffusion velocity $\frac{\sqrt{\beta g \Delta T L}}{\sqrt{Gr}} = \frac{\mu}{\rho L}$ as the characteristic velocity according to Davis [21],

where L is the equivalent annulus gap width. For the elliptical, triangular, and square cases, L is the difference between the radius of the outer cylinder and that of the circumscribed circle encompassing the inner shape.

As such, the following non-dimensionalized quantities are introduced:

$$x^* = \frac{x}{L}, y^* = \frac{y}{L}, u^* = \frac{uL\rho}{\mu}, v^* = \frac{vL\rho}{\mu}, w^* = \frac{vL\rho}{\mu}, Pr = \frac{\mu}{\alpha\rho},$$

$$Ra = \frac{g\beta(T_i - T_o)L^3\rho}{\alpha\mu}, p^* = \frac{(p + \rho_\infty gy)L^2}{\rho(\mu/\rho)^2}, T^* = \frac{T - T_o}{T_i - T_o}$$

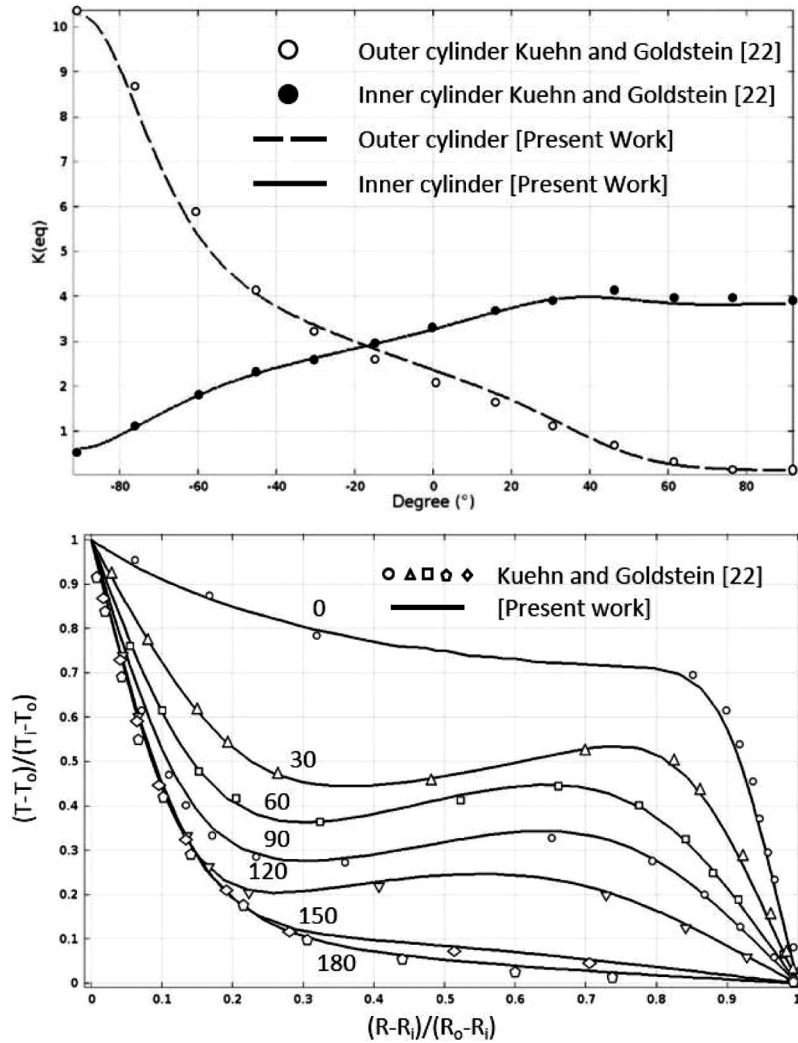


Figure 2. Comparison of the present results to those of Kuehn and Goldstein [22] at $Ra = 5 \times 10^4$: (a) Local equivalent conductivity along the inner and outer surfaces, (b) dimensionless radial temperature.

Table 3. Comparison of the average heat transfer results for a cylindrical annulus to those of Kuehn and Goldstein [22]

Ra_L	Pr	L/D_i	Location	K_{eq}		Deviation %
				Present work	Kuehn and Goldstein [22]	
10^2	0.7	0.8	Inner	1.000	1.000	0
			Outer	1.001	1.002	0.1
10^3	0.7	0.8	Inner	1.081	1.081	0
			Outer	1.082	1.084	0.18
3×10^3	0.7	0.8	Inner	1.396	1.404	0.57
			Outer	1.396	1.402	0.43
6×10^3	0.7	0.8	Inner	1.714	1.736	1.2
			Outer	1.714	1.735	1.2
10^4	0.7	0.8	Inner	1.978	2.010	1.6
			Outer	1.979	2.005	1.3
2×10^4	0.7	0.8	Inner	2.374	2.405	1.3
			Outer	2.375	2.394	0.8
3×10^4	0.7	0.8	Inner	2.624	2.661	1.4
			Outer	2.625	2.643	0.7
5×10^4	0.7	0.8	Inner	2.957	3.024	2.2
			Outer	2.958	2.973	0.5
7×10^4	0.7	0.8	Inner	3.191	3.308	3.5
			Outer	3.193	3.226	1

Utilizing the above non-dimensionalized quantities the conservation of mass, momentum, and energy equations can be presented as:

$$\frac{\partial u^*}{\partial x^*} + \frac{\partial v^*}{\partial y^*} = 0 \tag{1}$$

$$u^* \frac{\partial u^*}{\partial x^*} + v^* \frac{\partial u^*}{\partial y^*} = -\frac{\partial p^*}{\partial x^*} + \frac{\partial^2 u^*}{\partial x^{*2}} + \frac{\partial^2 u^*}{\partial y^{*2}} \tag{2}$$

Table 4. Comparison of the average heat transfer results for a square inner configuration to those of Chang et al. [23]

Aspect ratio	Ra	K_{eq}		Deviation %
		Present work	Chang et al. [23]	
0.2	10^3	1.027	1.003	2.4
	5×10^3	1.353	1.346	0.5
	10^4	1.648	1.644	0.2
	5×10^4	2.452	2.457	0.2
	10^5	2.837	2.846	0.3
0.4	10^3	1.002	1.002	0.03
	5×10^3	1.049	1.043	0.5
	10^4	1.140	1.126	1.2
	5×10^4	1.687	1.617	4.3
	10^5	2.007	1.991	0.8

$$u^* \frac{\partial v^*}{\partial x^*} + v^* \frac{\partial v^*}{\partial y^*} = -\frac{\partial p^*}{\partial y^*} + \frac{\partial^2 v^*}{\partial x^{*2}} + \frac{\partial^2 v^*}{\partial y^{*2}} + \frac{Ra}{Pr} T^* \quad (3)$$

$$u^* \frac{\partial T^*}{\partial x^*} + v^* \frac{\partial T^*}{\partial y^*} = \frac{1}{Pr} \left(\frac{\partial^2 T^*}{\partial x^{*2}} + \frac{\partial^2 T^*}{\partial y^{*2}} \right) \quad (4)$$

The boundary conditions are expressed as:

$u^* = v^* = 0$ on the inner and outer walls,

$T^* = 1$ on the inner wall,

$T^* = 0$ on the outer wall.

2.2. Radiation Exchange

We increase the Raleigh number by increasing the temperature difference while keeping the other parameters fixed. As such when Ra increases, with the same reference temperature, radiation heat transfer becomes more prominent.

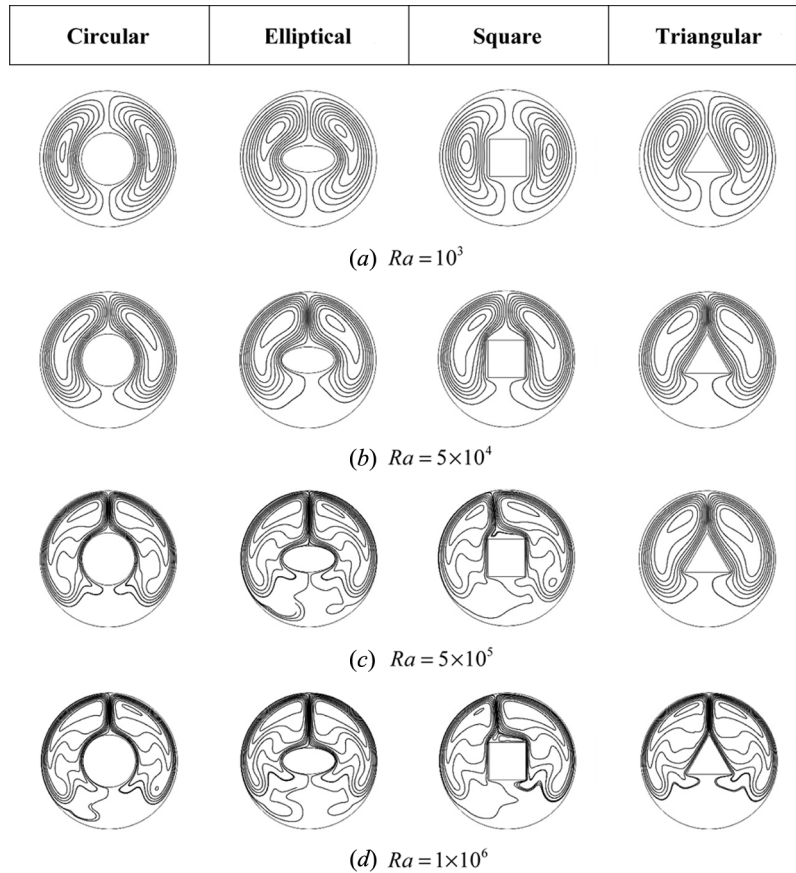


Figure 3. Streamlines in annuli of varying inner shape: Circular, elliptical, square, and triangular at different Rayleigh numbers.

In order to determine the total heat transfer at both inner and outer walls, we need to take into account both convection and radiation. In the present work, the local Nusselt number is used to include both convection and radiation contributions.

The local Nusselt number is expressed as:

$$Nu = Nu_c + Nu_r = \frac{q_c + q_r}{k(T_i - T_o)/L} \tag{5}$$

where q_c and q_r are local convective and radiative heat fluxes, respectively.

The total average Nusselt number, which includes the radiation contribution, is expressed as:

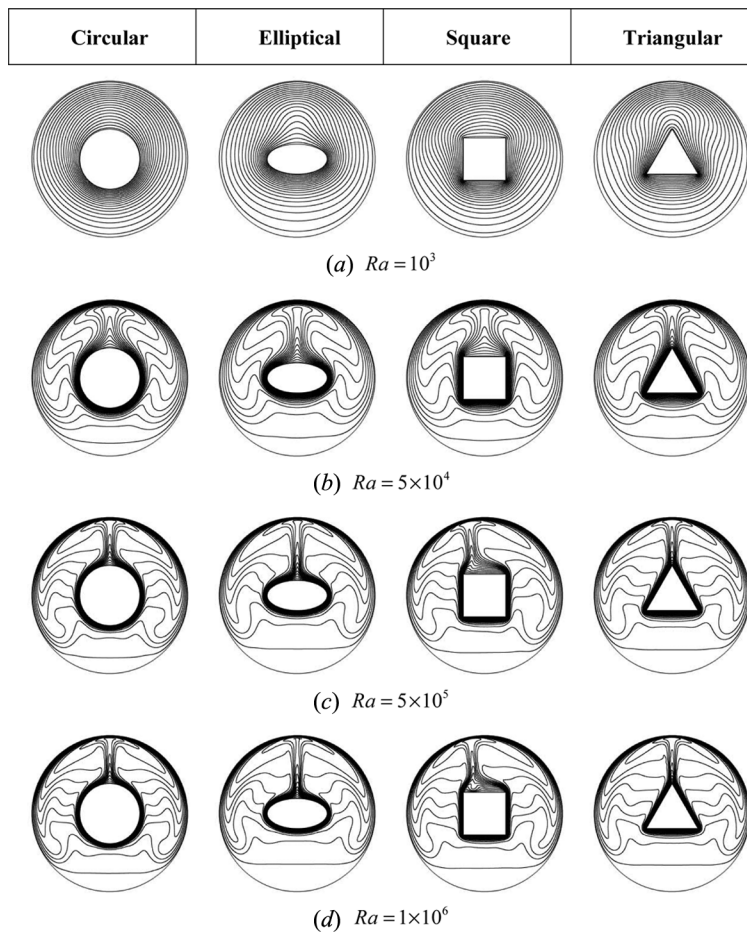


Figure 4. Isotherms in annuli of varying inner shape: Circular, elliptical, square, and triangular at different Rayleigh numbers.

$$\overline{Nu}_L = \overline{Nu}_c + \overline{Nu}_r = \frac{Q_c + Q_r}{Ak(T_i - T_o)/L} \tag{6}$$

where Q_c and Q_r are the total convective and radiative heat transfer, respectively along the surface.

3. VALIDATION

Figure 2(a) shows a comparison of the local equivalent conductivity (Nusselt number) to the results obtained by Kuehn and Goldstein [22]. As can be seen, a very good agreement is observed. Figure 2(b) shows a comparison of the dimensionless radial temperature profiles for air at $Ra = 5 \times 10^4$, $Pr = 0.7$ with those given in Kuehn and Goldstein [22]. The top vertical position is at 0° and the bottom curve at 180° . Once again a very good agreement is observed.

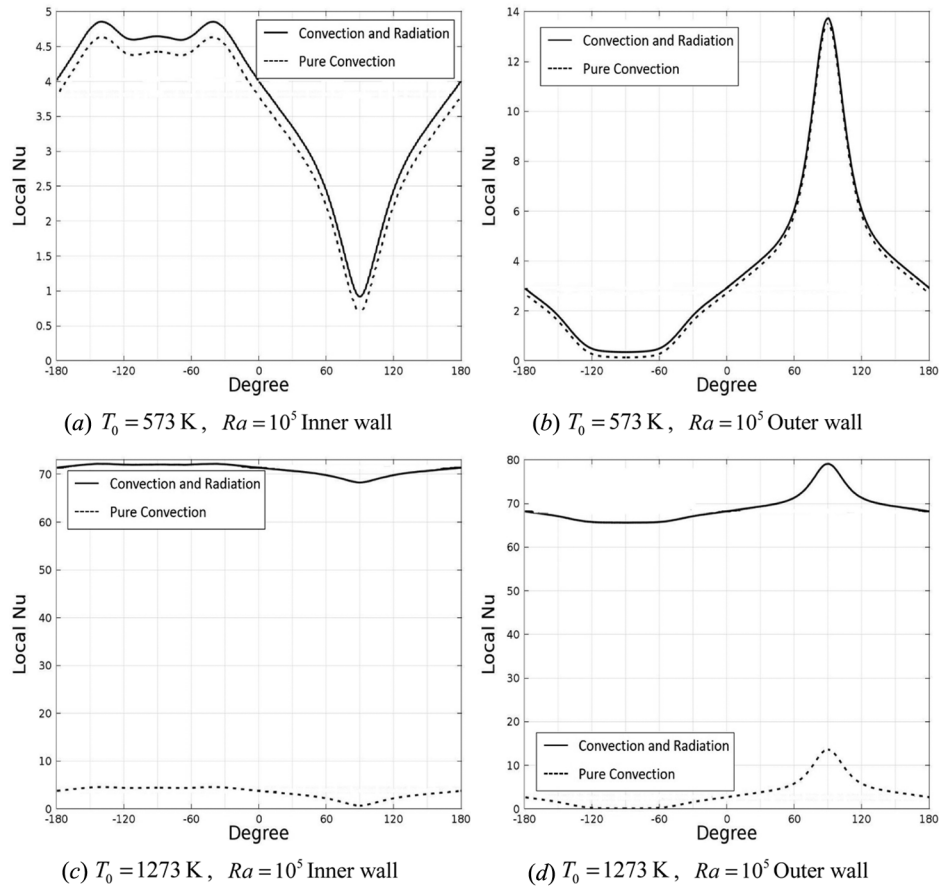


Figure 5. Comparison of local Nusselt number between pure convection and convection and radiation for a cylindrical annulus.

Comparison of the average heat transfer results to those of Kuehn and Goldstein [22] is given in Table 3. As can be seen, there is a very good agreement between the current results and those of Kuehn and Goldstein, with the average deviation being less than 0.999%.

Comparison of the average heat transfer results of the square inner configuration to those of Chang et al. [23] is given in Table 4. This shows a very good agreement between the current results for a square inner shape and those of Chang et al. (1983), with an average deviation of about 1.043%.

4. RESULTS AND DISCUSSION

The streamlines for an annulus composed of four nominal inner cross-sectional shapes, namely, circle, ellipse, square, and triangle at four different Rayleigh numbers are presented in Figure 3. As can be seen, the flow patterns for all four inner

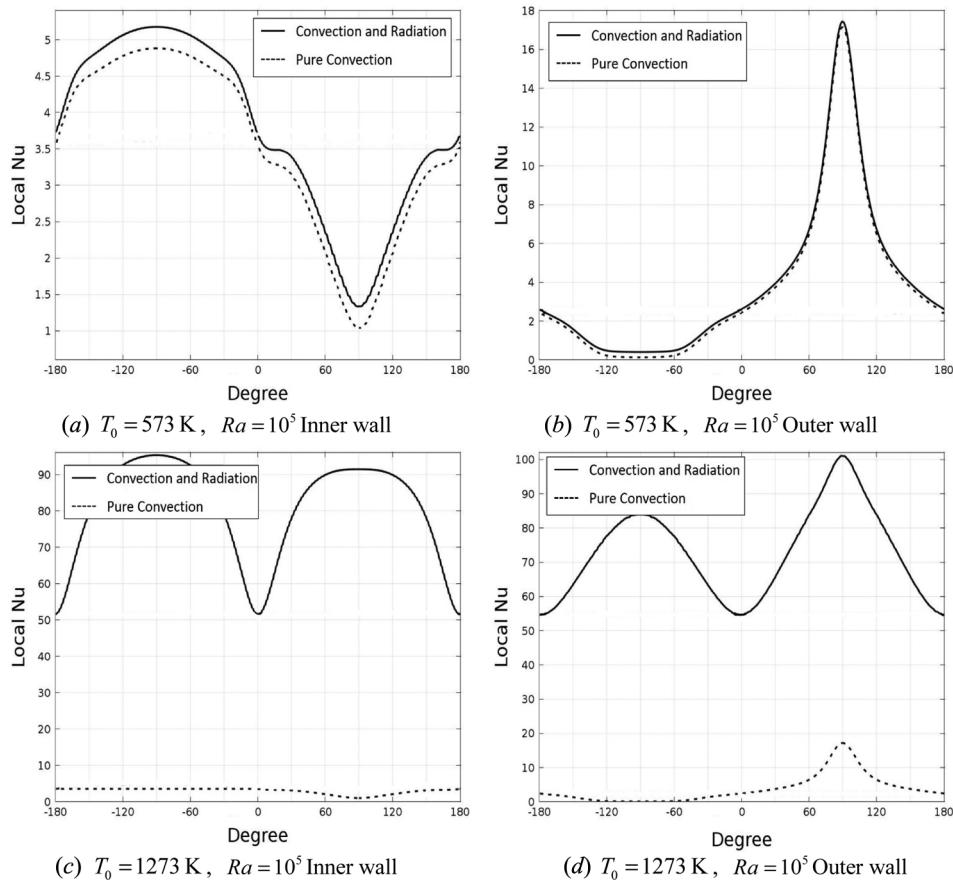


Figure 6. Comparison of local Nusselt number between pure convection and convection and radiation for an elliptical annulus.

shapes are somewhat similar. For low Rayleigh numbers, the flow is laminar in the annular region. The fluid near the inner hot surface moves upwards while that near the outer surface moves downwards. This recirculation occurs as the two boundary layers merge, creating the so called kidney-shaped core or cellular configuration.

As Rayleigh number increases the location of the configuration cell moves up, and when Ra reaches 5×10^5 , the flow begins to show unsteady characteristics which translates to asymmetric and distorted streamlines, as can be seen in Figure 3. Also as Rayleigh number increases, the circulation core is further confined at the top while forming a secondary core. At the same time, the width of both boundary layers diminishes.

The isotherms for these four different inner shapes annuli are given in Figure 4. For $Ra < 5 \times 10^4$, a symmetric pattern is observed for all four inner shapes. As expected, the square and triangular inner shapes show earlier distortion characteristics due to the presence of the corners for these geometries. The elliptical case also shows earlier distortion due to the larger top space. For higher Rayleigh

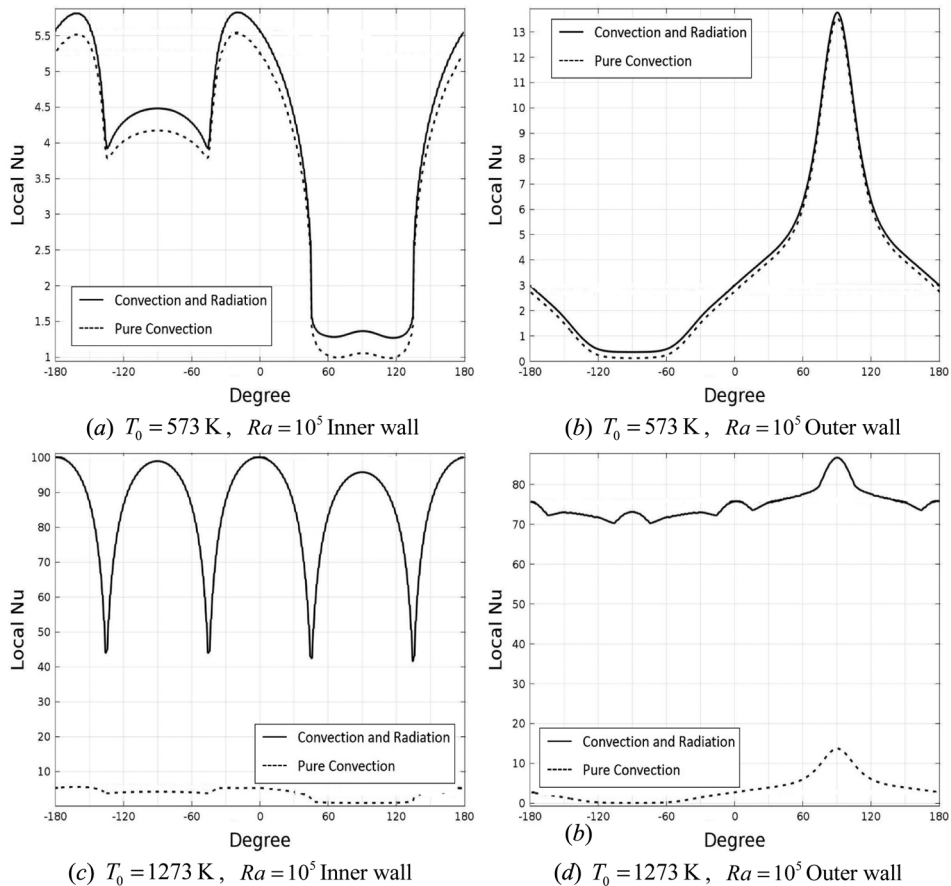


Figure 7. Comparison of local Nusselt number between pure convection and convection and radiation for a square annulus.

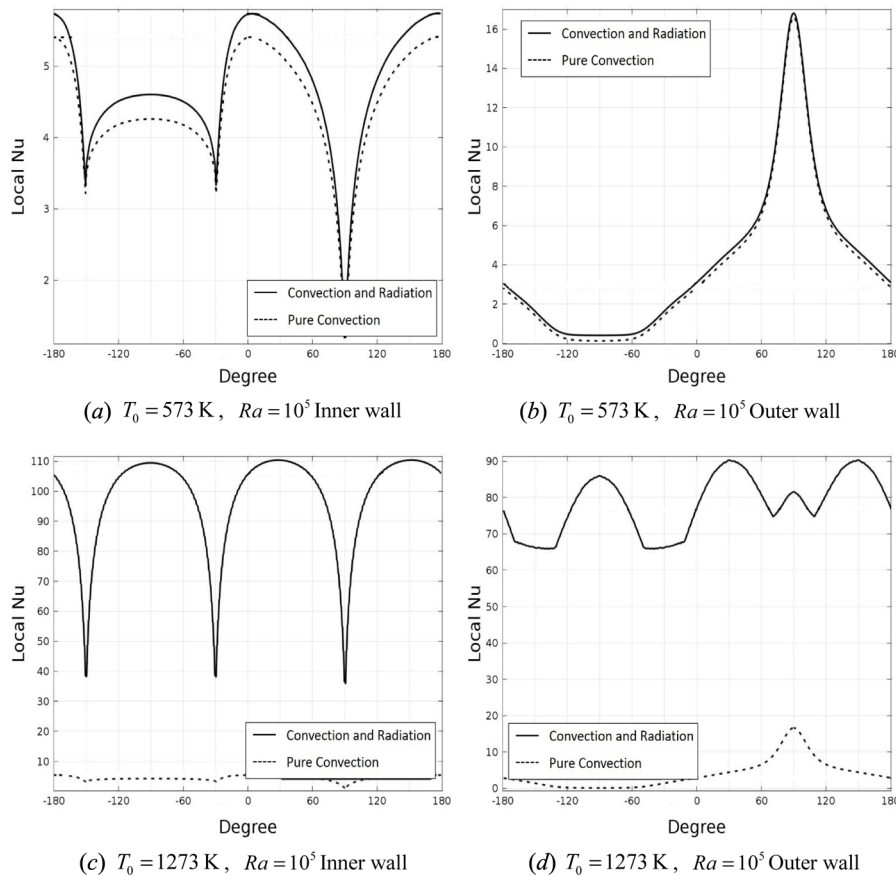


Figure 8. Comparison of local Nusselt number between pure convection and convection and radiation for a triangular annulus.

numbers, $Ra > 5 \times 10^4$, the square inner shape shows earlier signs of asymmetric characteristics.

Also for higher Rayleigh numbers, heat transfer becomes convection dominated as can be observed by the distorted isotherms and thinner boundary layers. At the same time, thermal stratification can be observed at $Ra = 10^6$. At higher Rayleigh numbers, the thermal boundary layer along the inner cylinder separates away from the top point and impinges on the outer cylinder around the top region. The fluid then flows near the outer cylinder towards the bottom, displaying the formation of a thermal plume. There also exists a temperature inversion in the region between the two boundary layers.

4.1. Local Nusselt Number

Figures 5–8 show a comparison between local Nusselt number for pure convection and that for convection and radiation for $T_0 = 573 \text{ K}$ and 1273 K at $Ra = 10^5$ for the four inner shapes.

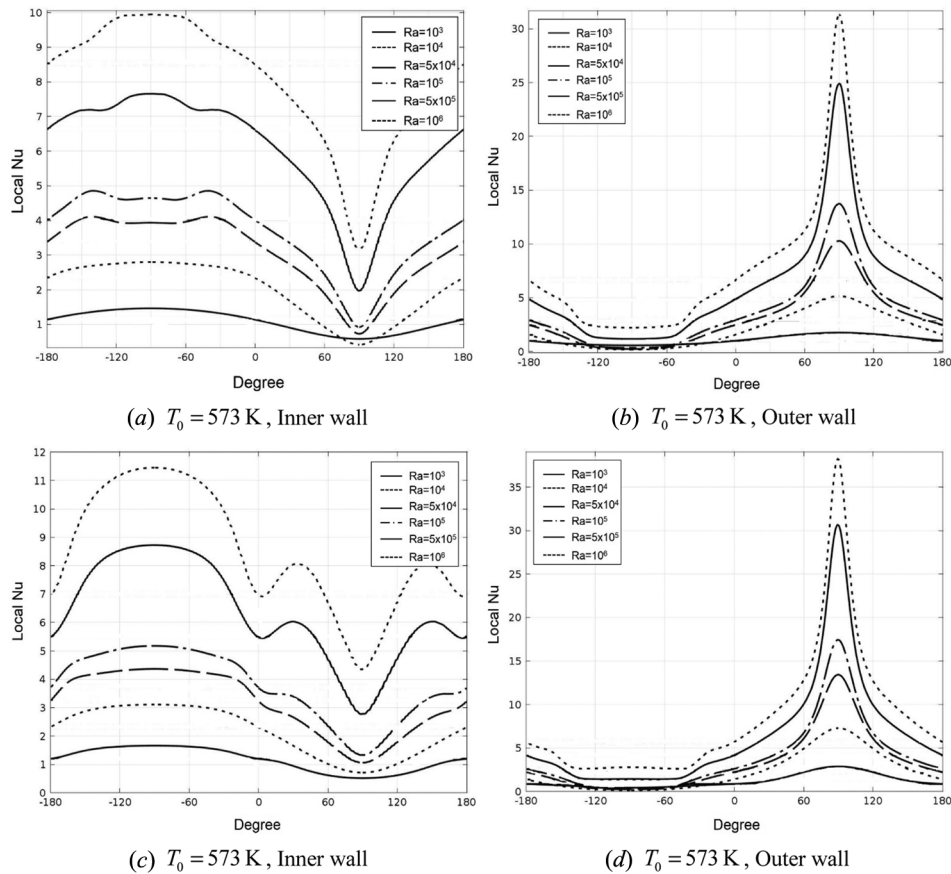


Figure 9. Effect of variation in Rayleigh number on Nusselt number distribution for cylindrical inner surface. (a) Inner wall, (b) outer wall elliptical inner surface, (c) inner wall, (d) outer wall.

For the inner cylindrical annulus, the inner cylinder boundary layer is similar to that near a single horizontal cylinder. The thickness of the boundary layer increases as the fluid flows upward. As such the thinnest boundary layer on the inner cylinder occurs at its bottom, which results in the steepest temperature gradient and maximum Nusselt number. The inner boundary layer impinges on the outer boundary layer, establishing the upper plume above the inner cylinder. Figures 5(a) and (b) display this behavior.

In Figure 6(b), it can be seen that the peak value of the local Nusselt number around the outer wall is higher in the elliptical case than in the other three cases at $T_0 = 573$ K and $Ra = 10^5$. In Figure 7(a), the low values of Nu can be observed between -135 and -45° , which corresponds to the bottom plate. In Figure 8(a), the local Nu is seen to be markedly impacted by the presence of the three corners and the bottom flat surface. Figures 7(a) and 8(a) show a wider difference between the radiation-added Nu and pure convection around the middle region of the flat surface.

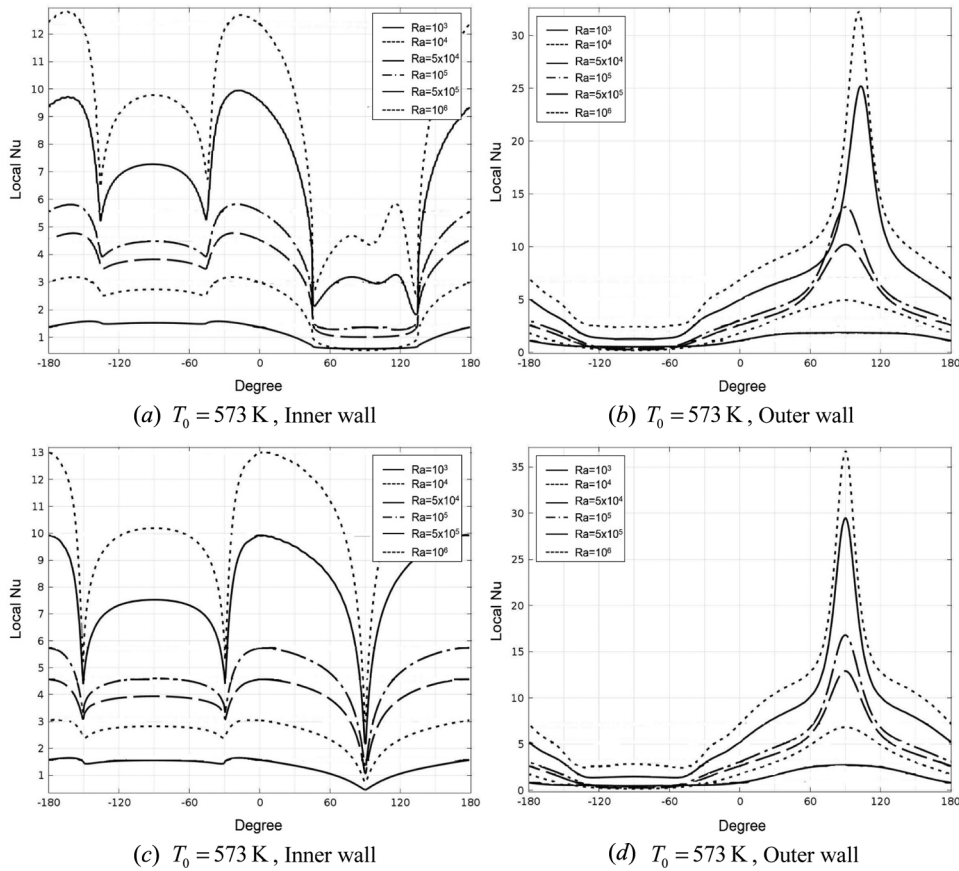


Figure 10. Effect of variation in Rayleigh number on Nusselt number distribution for square inner surface. (a) Inner wall, (b) outer wall triangular inner surface, (c) inner wall, (d) outer wall.

When $T_0 = 573$ K, as seen in Figures 5–8, the radiation effect on the local heat transfer coefficient is relatively weak especially along the outer wall. However, when $T_0 = 1273$ K, local heat transfer becomes radiation dominated as seen in Figures 5–8. Furthermore, for the square and triangular examples, more peaks exist in radiation-modified Nusselt number than in pure convection as can be seen in Figures 7(d) and 8(d). These peaks occur around -180 , -90 , 0 , and 90° respectively for the square inner example, and around -90 , 45 , and 135° for the triangular example.

The radiation-corrected Nusselt number distribution at different Rayleigh numbers for the four different inner shapes at $T_0 = 573$ K is shown in Figures 9 and 10, respectively. As expected, an increase in Rayleigh number results in higher Nusselt number as seen in Figures 9 and 10.

Comparison of radiation and convection local Nusselt number distribution for annuli of varying inner shape at a given Rayleigh number are shown in Figure 11. It

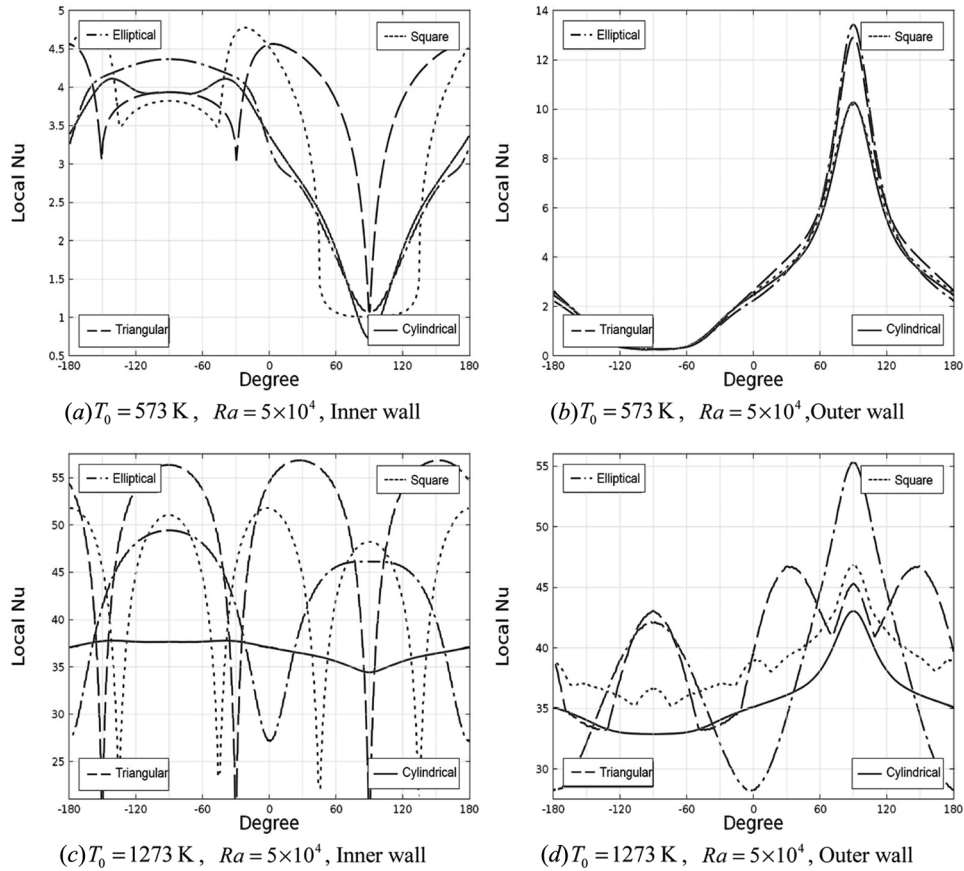


Figure 11. Comparison of Nusselt number distribution for different inner shapes at $Ra = 5 \times 10^4$. (a) and (b) $T_0 = 573 \text{ K}$; (c) and (d) $T_0 = 1273 \text{ K}$.

can be seen that the presence of corners and a larger top space enhances heat transfer performance.

As can be seen in Figure 11(a), local Nusselt number distribution along the inner surface is highest for the square annulus. However, the highest local value around the outer surface occurs with the elliptical annulus, as can be seen in Figure 11(b). As T_0 increases to 1273 K, it can be seen that the impact of radiation becomes substantially more dominant. Furthermore, for the elliptical, square, and triangular annuli, local Nusselt number shows a more prominent wavy trend in contrast to the cylindrical shape.

Figure 12 shows the effect of different radius ratios on local Nusselt number distribution, with $Ra = 1 \times 10^5$ and $T_0 = 1273 \text{ K}$. In the previous figures, the radius ratio, defined as R_o/R_i , was set at 2.6. In Figure 12, the local Nusselt distribution based on two different radius ratios is shown. As can be seen, the

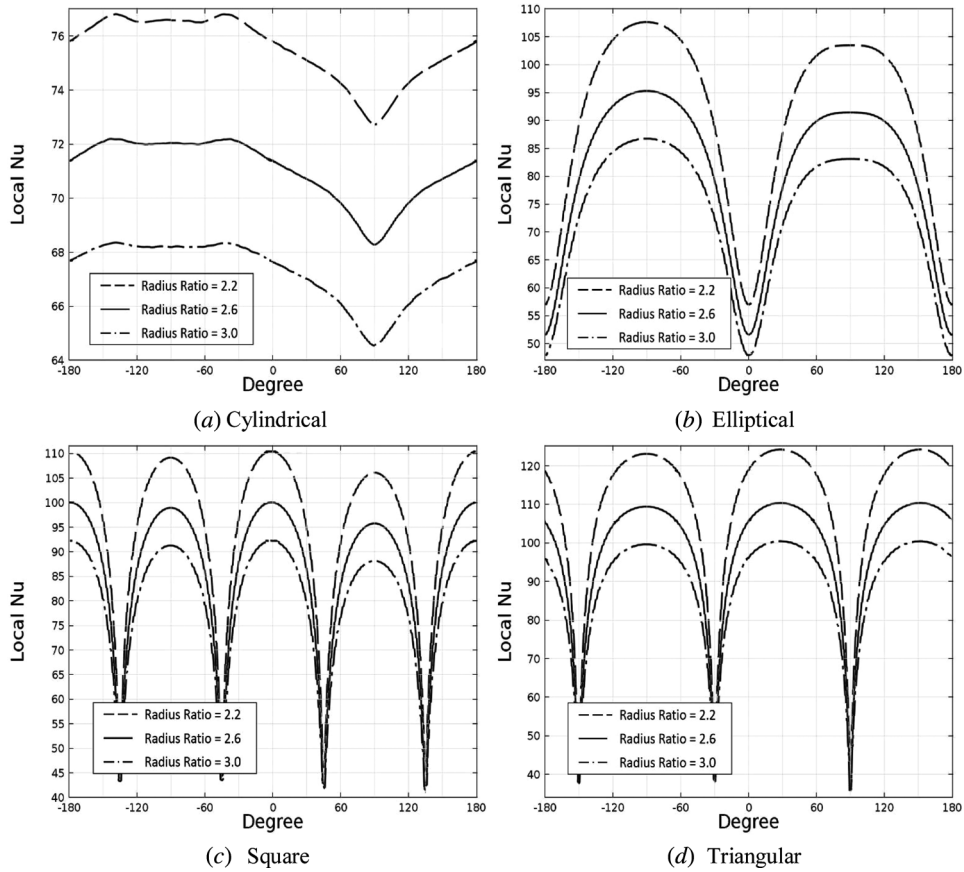


Figure 12. Comparison of Nusselt number distribution for different inner shapes at different radius ratios around the inner wall: $Ra = 1 \times 10^5$, $T_0 = 1273$ K.

lower radius ratio resulted in a higher Nusselt number in all four annulus configurations.

4.2. Heat Transfer Correlations

Heat transfer at any point in the domain is represented by the local Nusselt number, and the thermal radiation contribution within the annulus is incorporated in the total average Nusselt number as defined in Eq. (6).

Using many simulation runs, we established correlations for all four annulus configurations in terms of Rayleigh number dependence and at three pertinent reference temperatures. Since the total average Nusselt number at the inner shape entity is almost the same (<1% difference) as the absolute of that at the outer cylinder, we only present the inner shape average Nusselt number correlations in Table 5.

Table 5. Total average Nusselt number correlations at the inner surface for different inner shapes

Inner shape	Correlation	Conditions	Ra Range
Cylindrical	$\overline{Nu}_L = 0.2797 Ra_L^{0.2189}$	$T_0 = 293 \text{ K}$ Pr : 0.703	$\Delta T = Ra \cdot 9.6356 \times 10^{-9}$
	$\overline{Nu}_L = 0.1173 Ra_L^{0.3024}$	$T_0 = 573 \text{ K}$ Pr : 0.674	$\Delta T = Ra \cdot 2.0233 \times 10^{-7}$
	$\overline{Nu}_L = 0.0008 Ra_L^{0.9884}$	$T_0 = 1273 \text{ K}$ Pr : 0.719	$\Delta T = Ra \cdot 5.6569 \times 10^{-6}$
Square	$\overline{Nu}_L = 0.3203 Ra_L^{0.2094}$	$T_0 = 293 \text{ K}$ Pr : 0.703	$\Delta T = Ra \cdot 9.6356 \times 10^{-9}$
	$\overline{Nu}_L = 0.1241 Ra_L^{0.3005}$	$T_0 = 573 \text{ K}$ Pr : 0.674	$\Delta T = Ra \cdot 2.0233 \times 10^{-7}$
	$\overline{Nu}_L = 0.0009 Ra_L^{0.9881}$	$T_0 = 1273 \text{ K}$ Pr : 0.719	$\Delta T = Ra \cdot 5.6569 \times 10^{-6}$
Triangular	$\overline{Nu}_L = 0.3201 Ra_L^{0.2199}$	$T_0 = 293 \text{ K}$ Pr : 0.703	$\Delta T = Ra \cdot 9.6356 \times 10^{-9}$
	$\overline{Nu}_L = 0.1341 Ra_L^{0.3036}$	$T_0 = 573 \text{ K}$ Pr : 0.674	$\Delta T = Ra \cdot 2.0233 \times 10^{-7}$
	$\overline{Nu}_L = 0.001 Ra_L^{0.984}$	$T_0 = 1273 \text{ K}$ Pr : 0.719	$\Delta T = Ra \cdot 5.6569 \times 10^{-6}$
Elliptical	$\overline{Nu}_L = 0.3221 Ra_L^{0.2109}$	$T_0 = 293 \text{ K}$ Pr : 0.703	$\Delta T = Ra \cdot 9.6356 \times 10^{-9}$
	$\overline{Nu}_L = 0.1359 Ra_L^{0.2939}$	$T_0 = 573 \text{ K}$ Pr : 0.674	$\Delta T = Ra \cdot 2.0233 \times 10^{-7}$
	$\overline{Nu}_L = 0.0009 Ra_L^{0.9831}$	$T_0 = 1273 \text{ K}$ Pr : 0.719	$\Delta T = Ra \cdot 5.6569 \times 10^{-6}$

5. CONCLUSIONS

An investigation of natural convection in horizontal concentric annuli of varying inner shape was presented in this work. The effects of variation in inner shape on the flow field and heat transfer characteristics were analyzed. Also, the effect of surface radiation was incorporated in our investigation. Our model was validated against a number of pertinent results in the open literature.

The presence of corners in the square and triangular annuli and the larger top space in the elliptical annulus was found to enhance heat transfer performance as compared with that in the cylindrical annulus. Radiation was found to play an important role in the overall heat transfer behavior in natural convection at higher temperature levels. We also established correlations for total average Nusselt number, including surface radiation.

REFERENCES

1. D. Angeli, G. S. Barazzi, M. W. Collins, and O. M. Kamiyo, A Critical Review of Buoyancy-Induced Flow Transitions in Horizontal Annuli, *Int. J. Therm. Sci.*, vol. 49, pp. 2231–2241, 2010.
2. C. J. Ho, Y. H. Lin, and T. C. Chen, A Numerical Study of Natural Convection in Concentric and Eccentric Horizontal Cylindrical Annuli with Mixed Boundary Conditions, *Int. J. Heat Fluid Flow*, vol. 10, pp. 40–47, 1989.
3. C. Shu, Q. Yao, K. S. Yeo, and Y. D. Zhu, Numerical Analysis of Flow and Thermal Fields in Arbitrary Eccentric Annulus by Differential Quadrature Method, *Heat Mass Transfer*, vol. 38, pp. 597–608, 2002.
4. C. Y. Han and S. W. Baek, Natural Convection Phenomena Affected by Radiation in Concentric and Eccentric Horizontal Cylindrical Annuli, *Numer. Heat Transfer Part A: Appl.*, vol. 36, pp. 473–488, 1999.
5. A. Shaija and G. S. V. L. Narasimham, Effect of Surface Radiation on Conjugate Natural Convection in a Horizontal Annulus Driven by inner Heat Generating Solid Cylinder, *Int. J. Heat Mass Transfer*, vol. 52, pp. 5759–5769, 2009.
6. Z. Tan and J. R. Howell, Combined Radiation and Natural Convection in a Two-Dimensional Participating Square Medium, *Int. J. Heat Mass Transfer*, vol. 34, pp. 785–793, 1991.
7. M. Akiyama and Q. P. Chong, Numerical Analysis of Natural Convection with Surface Radiation in a Square Enclosure, *Numer. Heat Transfer Part A: Appl.: An Int. J. Comput. Methodol.*, vol. 31, pp. 419–433, 1997.
8. N. B. Sambamurthy, A. Shaija, G. S. V. L. Narasimham, and M. V. K. Murthy, Laminar Conjugate Natural Convection in Horizontal Annuli, *Int. J. Heat Fluid Flow*, vol. 29, pp. 1347–1359, 2008.
9. X. Xu, G. Sun, Z. Yu, Y. Hu, L. Fan, and K. Cen, Numerical Investigation of Laminar Natural Convective Heat Transfer from a Horizontal Triangular Cylinder to its Concentric Cylindrical Enclosure, *Int. J. Heat Mass Transfer*, vol. 52, pp. 3176–3186, 2009.
10. X. Xu, Z. Yu, Y. Hu, L. Fan, and K. Cen, A Numerical Study of Laminar Natural Convective Heat Transfer Around a Horizontal Cylinder Inside a Concentric Air-filled Triangular Enclosure, *Int. J. Heat Mass Transfer*, vol. 53, pp. 345–355, 2010.
11. Z. Yu, L. Fan, Y. Hu, and K. Cen, Prandtl Number Dependence of Laminar Natural Convection Heat Transfer in a Horizontal Cylindrical Enclosure With an Inner Coaxial Triangular Cylinder, *Int. J. Heat Mass Transfer*, vol. 53, pp. 1333–1340, 2010.

12. R. D. Boyd, Interferometric Study of Natural Convection Heat Transfer in a Horizontal Annulus with Irregular Boundaries, *Nucl. Eng. Des.*, vol. 83, pp. 105–112, 1984.
13. C. Shu, H. Xue, and Y. D. Zhu, Numerical Study of Natural Convection in an Eccentric Annulus Between a Square Outer Cylinder and a Circular Inner Cylinder Using DQ Method, *Int. J. Heat Mass Transfer*, vol. 44, pp. 3321–3333, 2001.
14. F. Moukalled, Natural Convection in the Annulus Between Concentric Horizontal Circular and Square Cylinders, *J. Thermophys. Heat Transfer*, vol. 10, pp. 524–531, 1996.
15. M. Keyhani, F. A. Kulacki, and R. N. Christensen, Free Convection in a Vertical Annulus with Constant Heat Flux on the Inner Wall, *Trans. ASME*, vol. 105, pp. 454–459, 1983.
16. F. A. W. Hamad, Experimental Study of Natural Convection Heat Transfer in Inclined Cylindrical Annulus, *Solar & Wind Technol.*, vol. 6, pp. 573–579, 1989.
17. Y. T. Tsui and B. Tremblay, On Transient Natural Convection Heat Transfer in the Annulus Between Concentric – Horizontal Cylinders with Isothermal Surfaces, *Int. J. Heat Mass Transfer*, vol. 27, pp. 103–111, 1984.
18. K. Vafai and J. Etefagh, An Investigation of Transient Three-Dimensional Buoyancy-Driven Flow and Heat Transfer in a Closed Horizontal Annulus, *Int. J. Heat Mass Transfer*, vol. 34, pp. 2555–2570, 1991.
19. C. P. Desai and K. Vafai, An Investigation and Comparative Analysis of Two and Three Dimensional Turbulent Natural Convection in a Horizontal Annulus, *Int. J. Heat Mass Transfer*, vol. 37, pp. 2475–2504, 1994.
20. K. Vafai and C. P. Desai, Comparative Analysis of the Finite Element and Finite Difference Methods for Simulation of Buoyancy Induced Flow and Heat Transfer in Closed and Open Ended Annular Cavities, *Numer. Heat Transfer Part A*, vol. 23, pp. 35–59, 1993.
21. G. D. V. Davis, Natural Convection of Air in a Square Cavity: A Bench Mark Numerical Solution, *Int. J. Numer. Methods Fluids*, vol. 3, pp. 249–264, 1983.
22. T. H. Kuehn and R. J. Goldstein, An Experimental and Theoretical Study of Natural Convection in the Annulus Between Horizontal Concentric Cylinders, *J. Fluid Mech.*, vol. 74, pp. 695–719, 1976.
23. K. S. Chang, Y. H. Won, and C. H. Cho, Patterns of Natural Convection Around a Square Cylinder Placed Concentrically in a Horizontal Circular Cylinder, *J. Heat Transfer*, vol. 105, pp. 273–280, 1983.